Phys. Status Solidi A **206**, No. 8, 1898–1903 (2009) / **DOI** 10.1002/pssa.200881449

physica status solidi a
www.pss-a.com
applications and materials science

Structural changes and peculiarities of NiPdSi formation investigated by Raman and Auger spectroscopy

Aliaksandra Karabko*[,1], Anatoly Dostanko[1], JinFang Kong[2], and Wenzhong Shen[2]

[1] Electronic Techniques and Technologies Department, Belarusian State University of Informatics and Radioelectronics, 6 P. Brovki Str., 220013 Minsk, Belarus
[2] Laboratory of Condensed Matter Spectroscopy and Opto-Electronic Physics, Department of Physics, Shanghai Jiao Tong University, 200030 Shanghai, P. R. China

Received 17 September 2008, revised 19 December 2008, accepted 4 January 2009
Published online 24 July 2009

PACS 64.70.kd, 68.55.Ln, 68.60.Dv, 78.30.Er, 79.20.Fv, 81.05.Je

* Corresponding author: e-mail alkorobko@gmail.com, Phone: +375 172 2938507, Fax: +375 172 2922513

In this contribution we report on peculiarities of formation, structural and vibrational properties of compositional (alloying) nickel silicides such as NiPdSi. MicroRaman analysis has shown that NiPdSi films are thermally stable up to 900 °C, which is by 100 °C higher than that for pure NiSi films. Using Miedema's model we have calculated the heat of formation for NiPdSi to be by 4 kJ mol^{-1} smaller than that for pure NiSi. This demonstrates an essential role of Pd in the enhancement of thermal stability of NiSi and in retardation of $NiSi_2$ phase formation. Raman spectra registered for NiPdSi show the peaks at wavenumbers typical for NiSi, although red shifted, as well as new Raman peaks at 322 and 434 cm^{-1} reported recently [Karabko et al., J. Appl. Phys. **105**, 033518 (2009)]. We have assigned these two peaks to the compositional disorder, introduced by the presence of Pd alloy. By means of Auger electron spectroscopy (AES) we have determined the peculiarities of the element distribution and Pd diffusion in NiPdSi and NiSi films, which results in a slight lack of silicon in the stoichiometry of phases and exponential decay law of Pd distribution with temperature.

© 2009 WILEY-VCH Verlag GmbH & Co. KGaA, Weinheim

1 Introduction Considerable attention has recently been paid to nickel silicide, which is a promising contact material for shallow p–n junctions, CMOS structures [1], Schottky diodes [2] and even photovoltaic applications [3], due to its superior physical properties of low resistivity, low silicon consumption, low temperature of formation, etc [4]. Apart from the well-known difficulties of film agglomeration and morphological instability at 600–700 °C, one of the vital issues to be addressed is the improvement of the thermal stability and the delay of undesirable $NiSi_2$ phase formation. The key approaches in optimising the thermal stability of NiSi are related either to introduction of a thin interlayer or alloying with a small amount of other metals, namely refractory or noble metals. Recently, an optimisation of nickel silicide composition by the introduction of alloy elements, such as Pt, Zr, W, Mo and Pd [5, 6] has been found to become an effective way to reduce agglomeration, improve morphological and thermal stability of nickel monosilicide with temperature, and therefore to retard the formation of $NiSi_2$ phase. The introduction of Pt has been studied extensively [6–8], while there are significantly less works on the interesting topic of Pd and other metals incorporation, although the possibility of the improvement of the thermal stability of NiSi by an introduction of a thin Pd interlayer has been determined by XRD [8]. At the same time the presence of alloy elements during solid phase reaction between silicon and a thin Ni film at annealing can lead to lattice imperfections, defects and compositional disorder in the film, which are difficult to predict. Furthermore, the change of vibrational properties in materials with temperature can strongly depend on the alloy content and its distribution. Therefore, the fast and adequate methods for monitoring the variation of properties of nickel silicides, modified by 3rd element incorporation, are required. Such monitoring can be performed, for example, by microRaman and Auger electron spectroscopy (AES).

WILEY InterScience® DISCOVER SOMETHING GREAT

© 2009 WILEY-VCH Verlag GmbH & Co. KGaA, Weinheim

In this paper we present an effective comparison of structural and vibrational properties, and peculiarities of NiSi and NiPdSi formation.

2 Experimental In our study, Ni(Pd ~ 0, 10 at.%) thin films were deposited on n-type (111) Si substrates by dc magnetron sputtering system. The deposition temperature was room temperature. Generally, the addition of 5–10% of metal is considered enough to influence the thermal stability of silicide in Ni(M)Si alloy, although the addition of 10% delays the formation of nickel disilicide phase more efficiently [1]. The silicidation process was carried out in inert gas ambient in vacuum furnace in a two-step annealing process. The first annealing was carried out at 475 °C for 30 min to form NiPdSi with subsequent etching of unreacted metal. Annealing temperatures for the second annealing were varied from 600 to 900 °C and also for 30 min. MicroRaman spectra were obtained in a backscattering geometry of $z(x, -)\bar{z}$ on a Jobin Yvon LabRam HR 800 UV microRaman system with Andor DU420 CCD detector using a 514.5 nm line of Ar^+ laser as an excitation source at room temperature. AES measurements were conducted on Perkin Elmer spectrometer PHI-660 also at room temperature.

3 Results and discussion

3.1 Raman measurements Figure 1 presents the room temperature microRaman spectra of NiPd films on Si substrates, annealed at various temperatures. The inset in Fig. 1 displays spectra for the pure Ni films on Si substrates at the same annealing conditions, which are in good agreement with the earlier reports [9, 10]. For NiPdSi samples we can clearly observe the presence of NiSi phase, with the major Raman peaks at 193, 210, 292 and 362 cm^{-1} of various intensities in the annealing temperature range of 600–850 °C (Fig. 1). The detailed Raman spectra analysis for NiPdSi and NiSi films is reported elsewhere [11]. The red shift of the peaks at 193 and 210 cm^{-1} is found in comparison with the pure NiSi samples, where the same peaks occur at 196 and 214 cm^{-1}. The introduction of Pd increases the interatomic distance in crystalline lattice, which in turn shifts the vibrational peak positions to lower frequencies. The frequency shift for the first-order peaks in NiPdSi samples due to the presence of 10% of Pd in Ni film can be roughly estimated from the mass change point of view [12]:

$$\omega \cong \omega_{NiSi} \left(\frac{\mu_{NiSi}}{\mu_{NiPdSi}} \right)^{1/2}, \quad (1)$$

with an assumption that in the particular mode the Ni and Pd atoms vibrate in phase against the Si atoms, like in an optic mode of a diatomic cubic crystal, so we could apply the simple effective mass formula. In Eq. (1) ω the shifted frequency, ω_{NiSi} the frequency for pure NiSi film, μ_{NiSi} and μ_{NiPdSi} the effective masses of NiSi and NiPdSi compounds, respectively. Values of $\omega = 192.1$ and 209.7 cm^{-1} can be yielded for the frequency shifts of 196 and 214 cm^{-1} modes, which are very close to the experimental results.

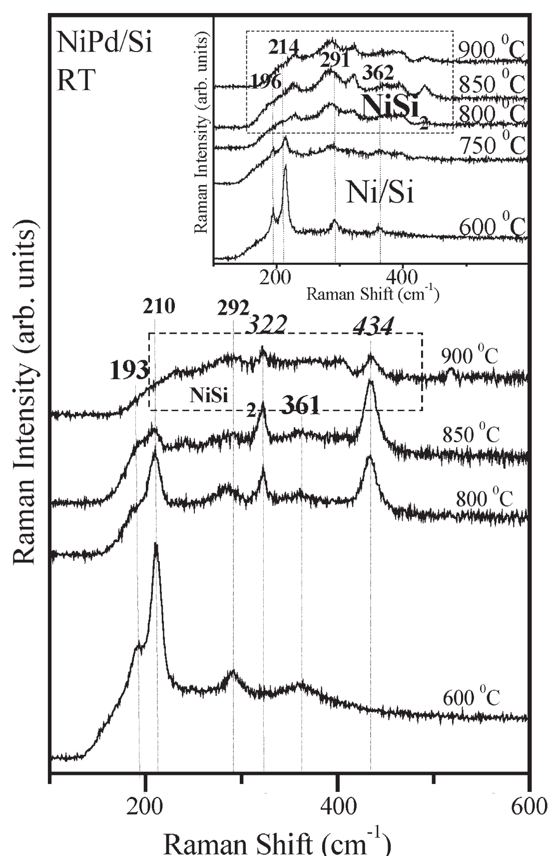

Figure 1 Room temperature microRaman spectra for NiPd and NiSi (inset) films on Si, annealed at various temperatures.

NiSi and NiPdSi films have proved to be polycrystalline in the result of experimental evaluation. As a matter of fact crystalline grains, oriented differently, influence the diffracted light and introduce the changes into Raman spectra [13]. By investigating Raman spectra and analysing the intensity ratio of the most intensive peaks (for NiPdSi and NiSi they are $I_{210\,cm^{-1}}/I_{193\,cm^{-1}}$ and $I_{214\,cm^{-1}}/I_{196\,cm^{-1}}$, respectively), one can qualitatively evaluate the degree of epitaxy of the film at microscopic level [13]. From Fig. 1 it is estimated that the intensity ratio changes from 1.62 to 4.25 for NiSi films, and from 1.07 to 2.85 for NiPdSi films, which reveals that there are grains of different orientations. Moreover, we can conclude that NiPdSi films are more homogeneous as the dispersion of the relative intensity values is smaller.

As was recently reported in our paper [11], two additional peaks at 322 and 434 cm^{-1} appear in Raman spectra of NiPdSi and these peaks become more pronounced with increase of temperature to 900 °C. These two phonon peaks can be attributed to the disorder Raman effects induced by the introduction of Pd element. As it is known, structural and compositional disorder in films may arise from contributions of dilute impurities, alloys, vacancies, defect complexes,

© 2009 WILEY-VCH Verlag GmbH & Co. KGaA, Weinheim

anharmonicity, as well as from mass variation [14]. In fact, the presence of the alloy introduces the defects to the films, which could lead to the breakage of translational symmetry, which results in the appearance of more peaks in Raman spectra. In comparison, the peaks at similar positions are detected in pure NiSi films when the transformation to $NiSi_2$ phase is already fully completed (Fig. 1 (inset), 850 °C), where the disorder-induced Raman scattering arises from the transformation of the crystal lattice in the films. It is likely to be assigned to Si-site disorder associated with either or both Ni-antisite defects on Si sites and Si vacancies [14].

From Fig. 1 it is clear that the introduction of Pd in NiSi retards the formation of $NiSi_2$ phase up to about 900 °C, where the NiSi peaks at 193 and 210 cm^{-1} disappear, accompanying with the appearance of broad and diffuse peaks in the range of 200–450 cm^{-1}, characteristic to $NiSi_2$ structures [10, 14]. For comparison the full transformation to $NiSi_2$ phase for NiSi sample already occurs at 800 °C as the first-order Raman peak at 214 cm^{-1} disappears, while under critical transition condition of 750 °C, we still have NiSi phase, although influenced by a certain amount of $NiSi_2$ as peak broadening can be observed (Fig. 1, inset). Hence, the introduction of only 10% of Pd to the initial nickel film can retard the formation of $NiSi_2$ phase up to 900 °C which is generally about 100–150 °C more than that for pure NiSi film.

Such microRaman measurements give the direct experimental evidence for the theoretical predictions in frames of nucleation theory which is used to explain the enhancement of nickel monosilicide stability by addition of various alloy elements [2, 3, 5]. NiSi with the presence of Pd forms a solid state solution $Ni_{1-x}Pd_xSi$. Since the decrease in Gibb's free energy is smaller for $Ni_{1-x}Pd_xSi$ solid solution than that for pure NiSi, we expect the larger activation energy for $NiSi_2$ nucleation. As a consequence, a higher formation temperature is needed to achieve $NiSi_2$ phase in alloying nickel silicides.

3.2 Calculation of heat of formation of silicides

To support the argument that NiPdSi phase is stable up to 900 °C and the retard of $NiSi_2$ phase formation occurs, we can further calculate the heat of formation of NiPdSi and NiSi. The enhancement of the thermal stability for a compositional nickel silicide such as NiPdSi can be explained by the comparison of the heats of formation of nickel monosilicide phase in NiPdSi and NiSi films. We have applied a semi-empirical Miedema's model to calculate the heat of formation of nickel monosilicide in NiPdSi film and to compare that with pure NiSi sample, although the heat of formation for NiSi films could be obtained directly. For NiPdSi films direct assessment is very difficult as we lack adequate thermodynamics data. Miedema's semi-empirical cellular model for metal cohesion is based on two parameters ϕ^* and $n_{ws}^{1/3}$ that are assigned to each atom [15, 16]. Miedema also assumes that there are two contributions to the heat of formation for a binary alloy system. One contribution is attractive and arises from charge transfer between neighbouring cells and is proportional to $-(\Delta\phi^*)^2$, the other contribution is repulsive and arises from a surface-tension term and is proportional to $(\Delta n^{1/3})^2$. The full description of Miedema's model can be found elsewhere [15, 16]. The resulting equation for evaluating the heat of formation for nickel monosilicide is [17]:

$$\Delta H = c_A f_B^A \frac{V_A^{2/3}}{(n_{wS}^{-1/3})_{av}} P \left[-(\Delta\phi^*)^2 + \frac{Q}{P}\left(\Delta n_{WS}^{1/3}\right)^2 - \frac{R}{P} \right] \quad (2)$$

with

$$f_B^A = c_B^S \left[1 + 8\left(c_A^S c_B^S\right)^2 \right], \quad (3)$$

$$c_A^S = \frac{c_A V_A^{2/3}}{c_A V_A^{2/3} + c_B V_B^{2/3}}, \qquad c_B^S = \frac{c_B V_B^{2/3}}{c_A V_A^{2/3} + c_B V_B^{2/3}} \quad (4)$$

where ΔH is the heat of formation, c_A, c_B are the concentration of (A) Si and (B) Ni, respectively, c_A^S, c_B^S are surface concentrations of Si and Ni, V_A, V_B are the molar volume of Si and Ni, $n_{ws}^{1/3}$ is the density of electrons at the boundary of Wigner–Seitz cells of pure atoms, ϕ^* is the chemical potential for pure elements, f_B^A is the multiplicative factor for ordered alloys, P, Q and R are constants. Here ϕ^* is expressed in V, V in cm^3, n_{ws} in density units (d.u., 1 d.u. $= 6 \times 10^{22}$ el cm^{-3}), ΔH in kJ mol^{-1}, P, Q/P, R/P are equal to 12.45 (the unit is found in Ref. [15]), 9.4 $V^2/(d.u.)^{2/3}$ and 2.1 V^2, respectively.

The values n_{ws} for pure atoms are mainly taken from Ref. [15]. Meanwhile Ref. [17] report, that such values could have been determined inaccurately as they are obtained by an empirical linear relation between the density of electrons at the boundary of Wigner–Seitz cell and the compressibility of the metal, and it is desirable to calculate them accurately for every new compound. To get more accurate values we have performed the calculation of n_{ws} by solving Thomas–Fermi–Dirac equation (TFD equation) for the above-mentioned elements. For many elements, including Pd, it has not been done thus far.

On the basis of Thomas–Fermi–Dirac model of the atom, the electron density of the atom could be described [18]:

$$n(x) = \frac{Z}{4\pi a_F^3} \left[\varepsilon + \left(\frac{y(x)}{x} \right)^{1/2} \right]^3 \quad (5)$$

where $r = a_F x$ is a distance from the nucleus, a_F determined as follows $a_F = a_0(9\pi^2/128Z)^{1/3} = (0.8853a_0/Z^{1/3})$, with $a_0 = 0.0529$ nm—Bohr radius. In the above-mentioned equations Z denotes the atomic number of the element, and ε

© 2009 WILEY-VCH Verlag GmbH & Co. KGaA, Weinheim

Table 1 Experimental and calculated values of electron density of pure atoms.

element	$n_{ws}^{1/3}$ (d.u.)	
	experimental [15]	calculated
Ni	1.500	1.410
Pd	1.750	1.842
Si	1.670	1.743

Table 2 Calculated heat of formation for pure and compositional nickel monosilicides.

compound	ΔH (kJ mol^{-1})
NiSi	−92.65
NiPdSi	−96.68
NiPtSi	−95.57

is a refinement, taking into account the exchange correlation:

$$\varepsilon = \left(\frac{3}{32\pi^2}\right)^{1/3} Z^{-2/3}, \tag{6}$$

$y(x)$ is called the Thomas–Fermi–Dirac function, and it satisfies TFD equation:

$$\frac{d^2 y}{dx^2} = x\left[\varepsilon + \left(\frac{y}{x}\right)^{1/2}\right]^3 \tag{7}$$

with the boundary conditions for atoms in solids $y(0) = 1$, $y(x_0) = x_0 y'(0)$. Using these boundary conditions, we have calculated electron densities n_{ws} of Ni, Pd, Si by TFD equations. The numerical values were obtained by mathematical modelling using the products Comsol Multiphysics and MATLAB 6.5. These calculated values and for comparison the experimental values of electron density are listed in Table 1.

From Table 1 it is obvious that the accuracy of theoretical calculation with experimental data is approximately 94–95%. It means that in future analysis of different additives to nickel silicide one can easily change the experimental evaluation of $n_{ws}^{1/3}$ into theoretical determination, which is less time consuming.

The results of calculations of the heat of formation for pure and compositional NiSi are presented in Table 2. We have considered the addition of about 10% of Pd to nickel film content. Also we have performed the calculation for the addition of 10% of Pt to nickel film content, the positive effect of introduction of which on the thermal stability of nickel silicide is already known [16].

The calculated heat of formation is proved to be 4 kJ mol^{-1} more negative for NiPdSi sample than that for NiSi, indicating a stronger Si-metal bonding between atoms in silicide, which is the reason for retardation of $NiSi_2$ formation. The more negative heat of formation, the more difficult NiSi is transformed to $NiSi_2$. It is necessary to note, that the heat of formation of NiPdSi film is even more negative than that of NiPtSi, which indicates that the introduction of the same amount of Pd is more effective for the enhancement of the thermal stability of nickel monosilicide.

3.3 Auger spectroscopy measurements Further, we have also performed a thorough analysis of element distribution profiles in NiPdSi and NiSi films, annealed in the range of temperatures 475–900 °C, by means of AES. AES measurements were carried out up to a depth twice as much as the thickness of a silicide layer to ensure we get the full information about the elements distribution in nickel silicide and silicon. In Fig. 2 some of AES spectra of NiSi and NiPdSi films, namely annealed at 475 and 750 °C, are shown. At 475 °C for NiSi film, the composition of elements is uniform, and elements are homogeneously distributed throughout the formed silicide layer, while for NiPdSi film one can note at least two different compositions of elements in the silicide layer. At this annealing condition, the maximum of Pd

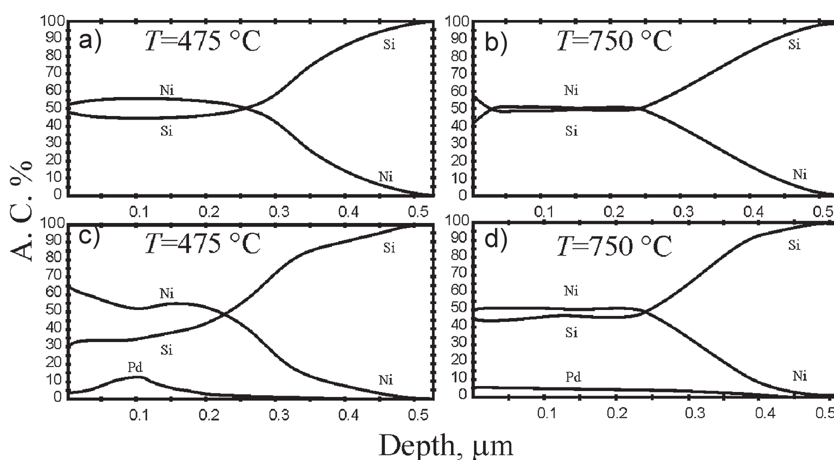

Figure 2 Auger spectra of (a, b) NiSi and (c, d) NiPdSi films, annealed at different temperatures.

© 2009 WILEY-VCH Verlag GmbH & Co. KGaA, Weinheim

distribution is found at about 0.1 μm for this sample. This could be explained by the fact that the initial thickness of the deposited metal alloy layer was also about 0.1 μm, which means that at this length the interface between silicon and the metal film has occurred. By solid phase formation process such interface becomes often the main source of defects and impurity localisation during the beginning stages of annealing. At 750 °C AES results yield a composition of elements to be straight 50–50% throughout the formed silicide layer in NiSi sample. At the same time according to Raman measurements this temperature is regarded a critical transition temperature for pure NiSi, when both phases NiSi and $NiSi_2$ are observed, although $NiSi_2$ concentration is still small. As Raman measurements unambiguously identify the phase content, we can conclude that such discrepancies in Raman and AES results can be due to the deviation from the equilibrium stoichiometry in the compound to the slight lack of silicon and the excess of metal phase, which is unseen during Raman measurements. This also occurs for NiPdSi films, where at this temperature the element composition is 46% Si, 4% Pd and 50% Ni, which indicates as well the dominance of metal phase. Therefore, we can say, that there is a compositional disorder in both NiPdSi and NiSi samples to the side of the excess of a metal phase.

By comparing the phase transformation kinetics and the change in element distribution profiles we can assume that either such annealing conditions or the presence of Pd result in the extra sedimentation of a small quantity of nickel metallic phase. It means that the silicides formed are not fully stoichiometric ideal.

The distribution of Pd in Si during NiSi solid phase reaction is known to be diffusion controlled [19] and obeys the exponential decay law of diffusion, which strongly depends on temperature and time of annealing. At lower annealing temperatures up to 700 °C, the distribution profile of Pd in NiSi layer can be described by Gauss function (Fig. 2c). At higher annealing temperatures, Pd becomes uniformly distributed throughout the silicide layer (Fig. 2d). Furthermore, the initial concentration of 10% of Pd in 100 nm nickel film is reduced to about 4% of equally distributed Pd in silicide film, changing with the temperature by exponential decay law (Fig. 3). The present Pd concentration was estimated as an average concentration of the element throughout the silicide layer.

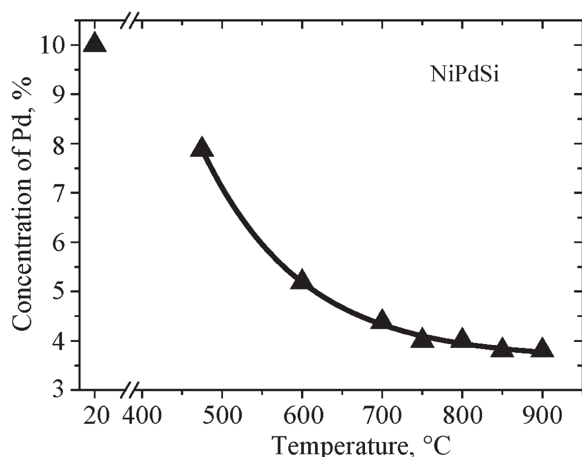

Figure 3 Dependence of the concentration of Pd in nickel silicide layer on annealing temperature. The solid line is obtained by fitting the data points with exponential decay function.

4 Conclusions The results of Raman and AES measurements have shown that the introduction of 10% of Pd in NiSi in comparison with pure NiSi films retards the formation of $NiSi_2$ by at least 100 °C and enhances the technology process window up to 900 °C. To support this argument we have calculated the heat of formation of NiPdSi according to Miedema's model to be 4 kJ mol^{-1} less than that of NiSi. Although this is a major advantage for the morphological and thermal stability of NiSi there are some peculiarities to note. Firstly, the presence of Pd introduces the redshift to the positions of NiSi vibrational peaks in Raman spectra, as it increases the interatomic distance of the crystal lattice in the film. In addition, we have noted two extra Raman peaks at 322 and 434 cm^{-1} in NiPdSi spectra gradually becoming more prominent with the increase of annealing temperature that can be attributed to the structural disorder, induced by Pd. Finally, we have investigated the element distribution in NiSi and NiPdSi films at various annealing temperatures and followed the diffusion of Pd element. The results of AES indicate that there is a deviation from the equilibrium stoichiometry with a slight lack of silicon and an excess of metal phase in the compound. At the same time Raman measurements, performed at the same annealing conditions, unambiguously confirm the presence of NiSi phase. Pd distribution with temperature is determined by exponential decay law, with Pd becoming uniformly distributed throughout NiSi layer with the total layer concentration of 4% only at 750 °C.

Acknowledgements A. O. Karabko would like to acknowledge the China Scholarship Council for providing the study and research grant. This work was supported by Ministry of Education of Belarus Grant 08-3076 and the Natural Science Foundation of China under contracts 10734020 and 10674094. We thank V. Ukhov for AES measurements assistance.

References

[1] C. Lavoie, F. M. d'Heurle, C. Detavernier, and C. Cabral, Jr., Microelectron. Eng. **70**, 144 (2003).
[2] K. J. Jin, K. L. Pey, W. K. Choi, D. A. Antoniadis, E. A. Fitzgerald, and D. Z. Chi, Thin Solid Films **504**, 149 (2006).
[3] D. S. Kim, E. J. Lee, J. Kim, and S. H. Lee, J. Korean Phys. Soc. **46**, 1208 (2005).
[4] W. Huang, L. Zhang, Y. Gao, and H. Jin, Microelectron. Eng. **84**, 678 (2007).
[5] D. Z. Chi, R. T. P. Lee, and A. S. W. Wong, Thin Solid Films **515**, 8102 (2007).
[6] C. Lavoie, C. Detavernier, C. Cabral, Jr., F. M. d'Heurle, and A. J. Kellock, Microelectron. Eng. **83**, 2042 (2006).

© 2009 WILEY-VCH Verlag GmbH & Co. KGaA, Weinheim

[7] D. Mangelinck, J. Y. Dai, J. S. Pan, and S. K. Lahiri, Appl. Phys. Lett. **75**, 1736 (1999).
[8] R. N. Wang and J. Y. Feng, J. Phys.: Condens. Matter **15**, 1935 (2003).
[9] S. K. Donthu, S. Tripathy, D. Z. Chi, and S. J. Chua, J. Raman Spectrosc. **35**, 536 (2004).
[10] F. F. Zhao, S. Y. Chen, Z. X. Shen, X. S. Gao, J. Z. Zheng, A. K. See, and L. H. Chan, J. Vac. Sci. Technol. B **21**, 862 (2003).
[11] A. O. Karabko, A. P. Dostanko, J. F. Kong, and W. Z. Shen, J. Appl. Phys. **105**, 033518 (2009).
[12] Y. H. Zhang, L. L. Guo, and W. Z. Shen, Mater. Sci. Eng. B **130**, 269 (2006).
[13] G. Conti, C. Lazik, and Y. Uritsky, Microsc. Microanal. **11**, 2094 (2005).
[14] F. Li, N. Lustig, P. Klosowski, and J. S. Lannin, Phys. Rev. B **41**, 10210 (1990).
[15] A. R. Miedema, P. F. deChatel, and F. R. de Boer, Physica B **100**, 1 (1980).
[16] J. R. Chelikowsky, Phys. Rev. B **25**, 6506 (1982).
[17] R. N. Wang, Y. He, and J. Y. Feng, Nucl. Instrum. Methods B **222**, 462 (2004).
[18] J. F. Liu, J. Y. Feng, and W. Z. Li, Nucl. Instrum. Methods B **194**, 289 (2002).
[19] S. P. Murarka, Silicides for VLSI Applications (Academic Press, New York, 1983).

© 2009 WILEY-VCH Verlag GmbH & Co. KGaA, Weinheim